J Math Chem (2014) 52:1831–1840
DOI 10.1007/s10910-014-0349-6

ORIGINAL PAPER

Effect of activation volume on the defect-induced anomalous electronic transport in $Rb_{0.8}Fe_2Se_2$

Rainer Kwang-Hua Chu

Received: 2 March 2014 / Accepted: 17 March 2014 / Published online: 12 April 2014

Abstract We adopted an absolute-reaction model which is considering the hole (defect)-induced charged frictionless transport to explain the unusual experiment: *Two single crystalline samples of the same nominal composition* $Rb_{0.8}Fe_2Se_2$ *were prepared using the self-flux technique via two different precursor routes. Although the difference in the final chemical composition falls within a narrow range, one was superconducting with a* $T_c \sim 31$ *K, while the other behaves like a narrow gap semiconductor*.

Keywords Absolute reaction · Boundary perturbation · Chemical proximity

1 Introduction

Discovery of charged superfluidity in $K_x(FeSe)_2$ ($T_c \sim 30$ K) [1] is one more step on the way to comprehend the mechanism of charged superfluidity in the family of layered Fe-based compounds (Fe-based chalcogenide [2]). Note that Fe (iron) itself under pressure is a superconductor with $T_c \sim 1.8$ K at 20 GPa [3]. After chemical doping with Se, FeSe becomes superconducting (SC) with $T_c = 8$ K and it has a simple PbO-type structure and a similarity to the critical $FeAs_4$-tetrahedra layers found in all iron-based superconductors [4].

Quite recently (within less than one year) successful intercalation of other alkali metals (Rb) in FeSe was realized and SC samples with T_c between 30 and 33 K were prepared [5–11]. Further studies of SC chalcogenides with hypothetical stoichiometry

R. K.-H. Chu (✉)
Department of Mathematics, School of Science, North University of China, Taiyuan 030051, P.R. China
e-mail: rainerkhchu@gmail.com

$Rb_{0.8}Fe_2Se_2$ revealed significant differences in their SC properties compared to the related SC pnictides with a similar structural arrangement (cf. [7–11]).

Note that when superconductive, a material has an electrical resistance of exactly zero. Superconductivity was discovered in 1911 by Heike Kamerlingh Onnes, who was studying the resistance of solid mercury at cryogenic temperatures using the recently-discovered liquid helium as a refrigerant. At the temperature of 4.2 K, he observed that the resistance abruptly disappeared [12]. All superconductors have exactly zero resistivity to low applied currents when there is no magnetic field present or if the applied field does not exceed a critical value.

In fact SC could be thought of as a charged superfluidity: Condensed electrons flow without energy dissipation [13]. However, as briefly introduced above, structural distortions under pressure and chemical doping in complicated compounds play important role for the onset of SC. The most interesting report is in Gooch et al. [11]: *Two single crystalline samples of the same nominal composition* $Rb_{0.8}Fe_2Se_2$ *were prepared using the self-flux technique via two different precursor routes following the same thermal history. Both samples display the same* $ThCr_2Si_2$*-structure with only slight differences in lattice parameters and the actual chemical composition as revealed by the WDS analysis. Although the difference in the final chemical composition falls within a narrow range, one was SC with a* $T_c \sim 30$ *K, while the other behaves like a narrow gap semiconductor*.

As remarked in Gooch et al. [11]: *The results suggest that superconductivity in this family of Fe-chalcogenides depends sensitively not just on doping as reflected in the chemical composition but also on the defects (Fe and/or Rb vacancies) and their state (ordered and/or disordered) present in the samples* (please cf. [9] or [7] for the latter issue). Based on this concern, in this short paper, we shall adopt the quantum chemistry approach [14–17] to investigate the defect(hole)-induced charged superfluidity considering especially previous measurements about $Rb_{0.8}Fe_2Se_2$ [11]. The theoretical part will be introduced in the next Section. Most of the theoretical details of our approaches could be traced in the verified reports [18–20] (especially [20] for the hole-induced onset of SC). In fact Eyring's idea: The free jumping of atoms or composite particles into the nearest neighboring vacancies through the kinetic zero-point motion (because these fluidized vacancies are moved about cooperatively by neighboring atoms or composite particles jumping into them, a vacancy confers gas-like degrees of freedom on three vibrational degrees of freedom) have successfully been applied to the study of quantum liquids (He-3 down to 1 K and He-4 down to 0.1 K with good comparison with experiments) [21,22]. Our focus will be on the onset temperature of the SC or charged superfluidity considering the almost zero resistance below the onset temperature. We shall demonstrate the effects of activation volume upon the defect-induced SC as well as the chemical doping about $Rb_yFe_{2-x}Se_2$ based superconductors.

2 Theoretical formulations

Eyring and Polanyi using the London equation provided a semi-empirical calculation of a potential energy surface (PES) of the $H+H_2$ reaction describing the journey of

nuclei from the reactant state of the system to the product state, passing through the crucial transition of activated complexes [14] (the birth of reaction dynamics). Subsequently the molecular theory of deformation kinetics came from a different stream of science than that of structure and motion of crystal defects (in particular dislocations). Its roots stretch to the developmental stages of theories of chemical reactions and thermodynamic description of their temperature dependence, culminating in the key formulation by Arrhenius of the equation for reaction rates (the transition-state (TS) theory is to assume the equilibration of the population between reactants and the transition state:

$$\mathbf{A}\ (\text{e.g., } Rb) + \mathbf{B}\ (\text{e.g., FeSe}) \leftrightarrow [\mathbf{TS}] \rightarrow \mathbf{products};$$

thus, the rate constant can be related to the equilibrium constant for formation of the transition state and hence the barrier energy (with the zero-point energy corrections) along the reaction coordinate [15,16]). Around the beginning of twentieth century the concept of activation entropy (reflects the change in vibrational modes perpendicular to the reaction coordinate) was included in the model, and it was considered that molecules go both in the forward direction (product state) and in the backward direction (reactant state).

We remind the readers that the development of statistical mechanics, and later *quantum mechanics*, led to the concept of the PES. This was a very important step in our modern understanding of microscopic models of deformation. The motion of composite particles is represented in the configuration space; on the potential surface the stable composite particles are in the valleys, which are connected by a pass that leads through the saddle point. A (composite) particle at the saddle point is in the transition (activated) state. Under the action of an applied stress the forward velocity of a flow unit is the net number of times it moves forward, multiplied by the distance it jumps. Eyring proposed a specific microscopic model of the amorphous structure and a mechanism of the flow [14–17]. A kind of (quantum) tunneling (possible between defects or holes) which relates to the matter rearranging by surmounting a potential energy barrier should occur during the microscopic deformation.

Note that in the transport of a (electronic) liquid or condensed state the motion of individual particles no longer dominates. A simple picture, according to Eyring [16], is that momentum transport is due to processes that involve the motion of vacancies or holes. These processes can be viewed as thermally activated transitions in which a particle or a cluster moves from one local energy minimum to another [18,19]. The viscosity of a liquid (condensed) state has a very strong dependence on temperature. As we shall illustrate the details below that the overall approach involves Planck's constant (h) [14–20]. The appearance of h is related to Eyring's assumption that the collision time of the composite particles is $h/(k_B T)$, the shortest timescale in a liquid or condensed state with k_B being the Boltzmann constant.

With the Eyring's TS model [14–17] (of stress-biased thermal activation), structural rearrangement is associated with a single energy barrier (height) E that is lowered or raised linearly by a shear (yield) stress τ. If the transition rate is proportional to the shear strain rate (with a constant ratio: $K_0 \approx 2V_a/V_m$), we can calculate the shear

stress or resistance ($\propto \rho_R$: the resistivity [19,20]) for the electronic fluid (or liquid)

$$\tau = \frac{E}{V_a} + \frac{k_B T}{V_a} \ln\left(\frac{\dot{\eta}}{K_0 \nu_0}\right), \tag{1}$$

where V_a is the activation volume, $\dot{\eta}$ is the shear strain rate, ν_0 is an attempt frequency [16,17], e.g., for temperatures (T) being $O(1)$ K: $\nu_0 \approx k_B/h \sim O(10^{11})$ (1/s). Normally, the value of V_a is associated with a typical volume required for a molecular shear rearrangement. Here $V_m = \lambda_2\lambda_3\lambda_1$, $\lambda_2\lambda_3$ is the cross-section of the transport unit on which the shear stress acts and λ_1 is the perpendicular distance between two neighboring layers of (composite) particles sliding past each other [16].

After using the forcing parameter Ψ (as the force balance gives the shear stress at a radius r as $\tau = -r\delta(\mathcal{F})/2$ with $\delta(\mathcal{F})$ being the net external forcing) we have (using the boundary perturbation series [18–20]) the forcing in terms of a referenced shearing stress (τ_0, via a ratio of a referenced energy and an activation volume) with

$$\Psi = -\left(\frac{r_2}{2\tau_0}\right)\delta(\mathcal{F}), \quad \delta(\mathcal{F}) = \delta(\rho_e E_z) \tag{2}$$

where r_2 is the mean outer radius of the cylindrical domain within which the electronic fluid (or liquid) transports through a thin shell region with a mean inner radius (r_1) [19], $\tau_0 = 2k_B T/V_a$, and $|-\delta(\rho_e E_z)|$ is the net electric force along the axis of the cylindrical domain or the transport direction, dp/dz is the pressure gradient along the axis, ρ_e is the net charge density, and E_z (the only electric field) is presumed to be a constant or uniform,

$$\dot{\eta} = \dot{\eta}_0 \sinh(\Psi) + \text{HOT} \tag{3}$$

with the small wavy-roughness effect being the first order perturbation which is rather small and thus neglected (HOT means the higher order contributions). Below is a brief explanation how to calculate $\dot{\eta}$ using the boundary perturbation approach (we set $\Psi \equiv \psi$).

2.1 Boundary perturbation

Along the outer interface (the same treatment below could also be applied to the inner interface of which it is not zero), we have $\dot{\eta} = (du/dn)|_{\text{on interfaces}}$. Here, n means the normal. Let u be expanded in ϵ:

$$u = u_0 + \epsilon u_1 + \epsilon^2 u_2 + \cdots,$$

and on the interface, we expand $u(r_0+\epsilon dr,\theta(=\theta_0))$ into

$$u(r,\theta)|_{(r_0+\epsilon dr,\,\theta_0)} = u(r_0,\theta)+\epsilon\,[dr\,u_r(r_0,\theta)]+\epsilon^2\left[\frac{dr^2}{2}u_{rr}(r_0,\theta)\right]+\cdots$$
$$= \left\{u_{slip}+\frac{\dot\eta r_2}{\psi}\left[\cosh\psi-\cosh\left(\frac{\psi r}{r_2}\right)\right]\right\}|_{\text{on interfaces}},\quad r_0\equiv r_2; \quad (4)$$

where

$$u_{slip}|_{\text{on interfaces}} = L_s^0\left\{\dot\eta\left[(1-\frac{\dot\eta}{\dot\eta_c})^{-1/2}\right]\right\}|_{\text{on interfaces}}, \quad (5)$$

Now, on the outer interface (cf. [18–20])

$$\dot\eta = \frac{du}{dn} = \nabla u\cdot\frac{\nabla(r-r_2-\epsilon\sin(k\theta))}{|\nabla(r-r_2-\epsilon\sin(k\theta))|} = \left[1+\epsilon^2\frac{k^2}{r^2}\cos^2(k\theta)\right]^{-\frac{1}{2}}\left[u_r|_{(r_2+\epsilon dr,\theta)}\right.$$
$$\left.-\epsilon\frac{k}{r^2}\cos(k\theta)u_\theta|_{(r_2+\epsilon dr,\theta)}\right] = u_{0_r}|_{r_2}+\epsilon[u_{1_r}|_{r_2}+u_{0_{rr}}|_{r_2}\sin(k\theta)$$
$$-\frac{k}{r^2}u_{0_\theta}|_{r_2}\cos(k\theta)]+\epsilon^2\left[-\frac{1}{2}\frac{k^2}{r^2}\cos^2(k\theta)u_{0_r}|_{r_2}+u_{2_r}|_{r_2}+u_{1_{rr}}|_{r_2}\sin(k\theta)\right.$$
$$\left.+\frac{1}{2}u_{0_{rrr}}|_{r_2}\sin^2(k\theta)-\frac{k}{r^2}\cos(k\theta)(u_{1_\theta}|_{r_2}+u_{0_{\theta r}}|_{r_2}\sin(k\theta))\right]+O(\epsilon^3). \quad (6)$$

Considering $L_s^0\sim r_2\gg\epsilon$ case, we also presume $\sinh\psi\ll\dot\eta_c/\dot\eta_0$. With equations above, using the definition of $\dot\eta$, we can derive the velocity field (u) up to the second order:

$$u(r,\theta) = -(r_2\dot\eta_0/\psi)\{\cosh(\psi r/r_2)-\cosh\psi\,[1+\epsilon^2\psi^2\sin^2(k\theta)/(2r_2^2)]$$
$$+\epsilon\psi\sinh\psi\,\sin(k\theta)/r_2\}+u_{slip}|_{r=r_2+\epsilon\sin(k\theta)}.$$

The key point is to firstly obtain the slip velocity along the boundaries or surfaces. After lengthy mathematical manipulations, we obtain the velocity fields (up to the second order) and then we can integrate them with respect to the cross-section (e.g., considering the regime: $R_1+\epsilon\sin(k\theta+\beta)\le r\le R_2+\epsilon\sin(k\theta)$) to get the transport (volume flow) rate (Q, also up to the second order here):

$$Q=\int_0^{\theta_p}\int_{R_1+\epsilon\sin(k\theta+\beta)}^{R_2+\epsilon\sin(k\theta)}u(r,\theta)r\,dr\,d\theta = Q_0+\epsilon\,Q_{p_0}+\epsilon^2\,Q_{p_2}.$$

In fact, the approximate (up to the second order) net transport (volume flux) rate reads:

$$
\begin{aligned}
Q = {} & \pi\dot{\eta}_0\{L_s^0(R_2^2 - R_1^2)\sinh\psi\,(1 - \frac{\sinh\psi}{\dot{\eta}_c/\dot{\eta}_0})^{-1/2} + \frac{R_2}{\psi}[(R_2^2 - R_1^2)\cosh\psi \\
& - \frac{2}{\psi}(R_2^2\sinh\psi \\
& - R_1R_2\sinh(\psi\frac{R_1}{R_2})) + \frac{2R_2^2}{\psi^2}(\cosh\psi - \cosh(\psi\frac{R_1}{R_2}))]\} + \epsilon^2\{\frac{\pi}{2}u_{slip_0}(R_2^2 - R_1^2) \\
& + L_s^0\frac{\pi}{4}\dot{\eta}_0\sinh\psi(1 + \frac{\sinh\psi}{\dot{\eta}_c/\dot{\eta}_0})(-k^2 + \psi^2)[1 - (\frac{R_1}{R_2})^2] + \frac{\pi}{2}\dot{\eta}_0[R_1\sinh(\frac{R_1}{R_2}\psi) \\
& - R_2\sinh\psi] \\
& - \frac{\pi}{2}\dot{\eta}_0\frac{R_2}{\psi}[\cosh\psi - \cosh(\psi\frac{R_1}{R_2})] + \frac{\pi}{4}\dot{\eta}_0\psi\cosh\psi[R_2 - \frac{R_1^2}{R_2}] \\
& + \pi\dot{\eta}_0\{[\sinh\psi + L_s^0\cosh\psi(1 + \frac{\sinh\psi}{\dot{\eta}_c/\dot{\eta}_0})](R_2 - R_1\cos\beta)\} + \frac{\pi}{2}\dot{\eta}_0\frac{R_2}{\psi}\cosh\psi \\
& + L_s^0\frac{\pi}{4}\psi^2\dot{\eta}_0\frac{\cosh\psi}{\dot{\eta}_c/\dot{\eta}_0}[1 - (\frac{R_1}{R_2})^2]\}\cosh\psi. \qquad (7)
\end{aligned}
$$

Here,

$$
u_{slip_0} = L_s^0\dot{\eta}_0\left[\sinh\psi\left(1 - \frac{\sinh\psi}{\dot{\eta}_c/\dot{\eta}_0}\right)^{-1/2}\right]. \qquad (8)
$$

The (referenced) shear rate is

$$
\dot{\eta}_0 = 2\frac{V_a}{V_m}\frac{k_BT}{h}\exp\left(\frac{-E}{k_BT}\right), \qquad (9)
$$

which is a function of temperature, the activation energy (E), the activation volume, and the length scale [16]. $K_0\nu_0$ in Eq. (1) is temperature dependent and the value could be traced in [18,20]. The remaining task is to fix the value of Ψ by prescribing r_2 and $|\delta(\rho_e E_z)|$ with different temperatures. Once the detailed or corresponding geometric scales in experimental setup were unknown (closely relevant to our formulations), we can select $|\delta(\rho_e E_z)| = 1$ (or $r_2 = 1$) for convenience. After all these, the remaining in the equation (1) is the unique relationship between V_a and T for a fixed τ ($\propto \rho_R$). Once we obtain the details of ρ_R ($\propto \tau$) vs. T then we can know which parameters are dominated. Note that most of the mathematical derivations could be found in the cited references of [18–20]. For instance, we can use our approach to identify the onset temperature of high-temperature superconductors (cf. [20]) after calibrating some physical as well as geometric parameters.

3 Numerical results and discussion

We firstly verify our approach by comparing our numerical results with those electrical resistivity (ρ_R) measurements considering chemical compound: $Rb_{0.8}Fe_2Se_2$ [11]. The relationship between ρ_R and τ could be traced in [20]. Figure 1 shows that there will be nearly frictionless or almost zero-resistance states ($\tau \propto \rho_R \sim 0$) if we select the activation energy to be 2×10^{-20} J. We can observe a starting (sharp) drop of the (electrical) resistance ($\propto \rho_R$) at $T \sim 31$ K ($V_a \approx 7.1 \times 10^{-24}\text{m}^3$) and there is almost zero resistance below 28 K ($V_a \approx 4.4 \times 10^{-24}\text{m}^3$). It illustrates there is a very low electrical resistivity around this temperature regime for selected physical parameters. Differenct symbols in Fig. 1 represent different activation volumes which are temperature dependent and are illustrated in Fig. 2. The qualitative as well as quantitative similarity are that this critical temperature (T_c) resembles that found in superconductor $Rb_{0.8}Fe_2Se_2$ [11] (cf. Fig. 2a for Sample A: The Wavelength Dispersive Spectrometer (WDS) analysis shows the chemical compositions are Rb/Fe/Se = 0.93(2)/1.70(2)/2.00 [11]). Note that from the expression of $|\tau| = [r\,\delta(\rho_e E_z)]/2$ (cf., e.g., [20]), with $r \neq 0$, we can understand that below T_c, as $\tau \sim 0$, the external forcing or electric-field could be absent (due to the persistent current occurring).

After verification of this chemical doping (or chemical pressure) effect, we shall demonstrate the effect due to a small amount of defects (considering vacancy or hole) on the transport of many electrons (cf. Fig. 2 in [20]). We remind the readers that it was remarked in Gooch et al. [11]: *Sample B behaves as a narrow-gap semiconductor as predicted*. The latter gives us the idea to find out the valid range of activation parameters before the time-consuming searching.

We illustrate the activation volume effect in Fig. 3. The activation energy is 2×10^{-20} Joule. We decrease the temperature from around 32 to around 15 K. The corresponding V_a for $T = 32$ and $T = 15$ K are 8×10^{-25} m^3 and 8×10^{-26} m^3, respectively. The resistivity ($\tau \propto \rho_R$, cf. [20]) increases exponentially as temperature decreases The trend is qualitatively similar to that reported in Fig. 2b (lower panel) of Gooch et al. [11] considering Sample B which has the same chemical compound

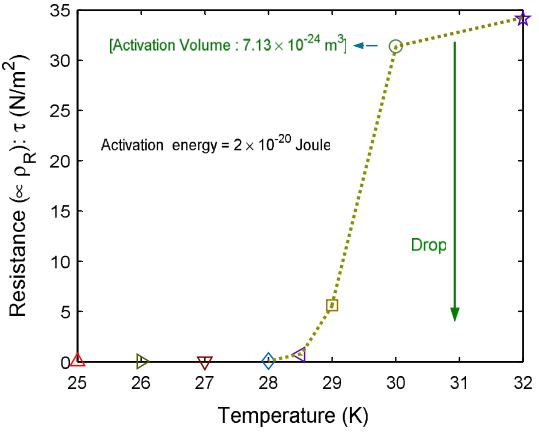

Fig. 1 Calculated resistance ($\propto \rho_R$ [20]) using an activation energy 2×10^{-20} J. There is a sharp decrease of resistance starting from around $T \sim 31$ K. Below around 28 K ($V_a \approx 4.4 \times 10^{-24}\text{m}^3$), the resistivity is almost zero. This critical temperature resembles that found in superconductor $Rb_{0.8}Fe_2Se_2$ (cf. Fig. 2a therein for Sample A) [11]

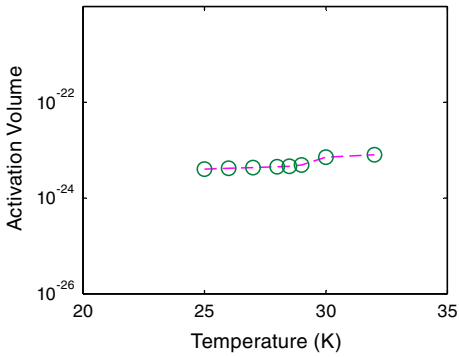

Fig. 2 Activation volume vs. temperature (K) and other parameters are the same as those in Fig. 1

as Fig. 1 above: $Rb_{0.8}Fe_2Se_2$ or with the same nominal compositions (Rb/Fe/Se = 0.8/2/2) for Fig. 1 above (note that the WDS analysis shows the chemical compositions Rb/Fe/Se = 0.90(1)/1.78(1)/2.00 [11]). Note that as reported in [7], considering $Rb_{0.85}(Fe_{1-y}Se)_2$, their data imply that the ordering of the vacancies in the FeSe layer may be present in both SC and non-superconducting states.

Before we give the short summary of our works here we like to make some remarks about our illustrations. We firstly remind the readers that the equivalence of zero resistivity and the Meissner effect has been derived in [23]. Our presented results, Figs. 1 and 2 are related to the Fig. 2a and b in Gooch et al. [11] which (resistivity) was measured without imposing external magnetic fields. Nevertheless the diamagnetic signal did appear for the Sample A under the zero-field-cooling. Meanwhile there is no diamagnetic signal for the Sample B [11]. Although we can here attribute the different electrical properties (two samples displaying the same crystal structure or the same nominal composition [11]) to the Eyring's hole- or defect-induced transport along the **nano-scale interface** [16,17,19,20] via the different activation volumes.

Other explanation [24] could also be valid: Due to the inhomogeneity in this system: $Rb_{0.8}Fe_2Se_2$. Note that it is possible as a whole the metallic phase (including the SC islands) coexists with the insulating regions. Due to the proximity effect the size of the SC regions should be of order or larger than the coherence length; otherwise, the SC state will be destroyed by the proximity contact with the normal matrix [24]. The latter could be the case of Sample B in Gooch et al. [11]. Meanwhile considering measurements of $Rb_{0.77}Fe_{1.61}Se_2$ ($T_c \sim 32.6$ K) [25] it was shown that the antiferromagnetic insulating phase is just a byproduct of Rb-intercalation and its magnetic properties have hardly any relation to the superconductivity. Borisenko *et al.* concluded that the key ingredient for superconductivity ($Rb_{0.77}Fe_{1.61}Se_2$) is a certain proximity of a van Hove singularity to the Fermi level [25]. We noticed that considering the effective D_{2d} symmetry for the chains of tetrahedra in the KFeS2 structures we have one distorted example: $RbFeSe_2$ and one undistorted example : $CsGaS_2$ (cf. Table 6 in [26]). Based on our above reasoning it is possible that the latter could be SC by partial replacement of Ga by S (with a more complex layer structure similar to the layer pnictides) or by pressurization at higher pressures.

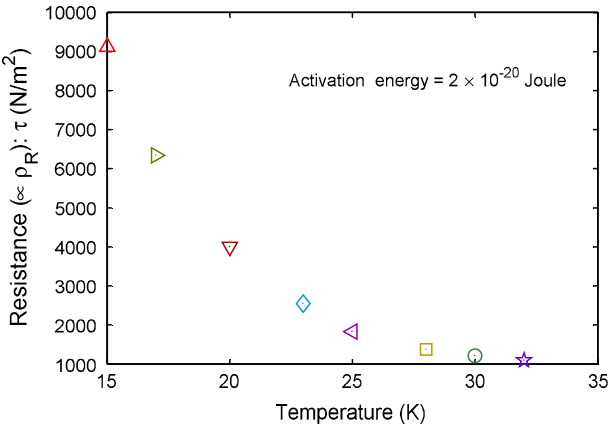

Fig. 3 Calculated resistance ($\propto \rho_R$ [20]) using an activation energy 2×10^{-20} J. The resistivity increases exponentially as temperature decreases (cf. Fig. 2b for Sample B in Gooch et al. [11]). This unusual behavior resembles that found in chemical compound: $Rb_{0.8}Fe_2Se_2$ with the same nominal compositions (Rb/Fe/Se = 0.8/2/2) for Fig. 1 above (note that the WDS analysis shows the chemical compositions Rb/Fe/Se = 0.90(1)/1.78(1)/2.00 [11])

4 Conclusion

To give a brief summary, we have adopted the TS approach (based on the quantum chemistry via the hole- or vacancy-induced transport developed by Eyring [16,19,20]) to study the hole(defect)-induced SC (considering $Rb_{0.8}Fe_2Se_2$ in Gooch et al. [11]). Our approaches can not only identify the onset temperatures of SC $Rb_{0.8}Fe_2Se_2$ based superconductors in Fig. 2a of Gooch et al. [11] considering the chemical doping effect but also, with the tuning of different activation volumes, demonstrate the possible semiconducting phase of $Rb_{0.8}Fe_2Se_2$ in Fig. 2b of Gooch et al. [11] at low-temperature range. Based on our results it is crucial to tune the activation volume (say, by carefully annealing and preparing of the samples) for increasing the SC temperature more effectively. We shall investigate other interesting issues in the future [27].

References

1. J.G. Guo, S.F. Jin, G. Wang, S.C. Wang, K.X. Zhu, T.T. Zhou, M. He, X.L. Chen, Superconductivity in the iron selenide KxFe2Se2 (0x1.0). Phys. Rev. B **82**, 180520(R) (2010)
2. Y. Mizuguchi, H. Takeya, Y. Kawasaki, T. Ozaki, S. Tsuda, T. Yamaguchi, Y. Takano, Transport properties of the new Fe-based superconductor. Appl. Phys. Lett. **98**, 042511 (2011)
3. K. Shimizu, T. Kimura, S. Furomoto, K. Takeda, K. Kontani, Y. Onuki, K. Amaya, Superconductivity in the non-magnetic state of iron under pressure. Nature **412**, 316 (2011)
4. F.-C. Hsu, J.-Y. Luo, K.-W. Yeh, T.-K. Chen, T.-W. Huang, P.M. Wu, Y.-C. Lee, Y.-L. Huang, Y.-Y. Chu, D.-C. Yan, M.-K. Wu, Superconductivity in the PbO-type structure alpha-FeSe. Proc. Nat. Acad. Sci. (USA) **105**, 14262 (2008)
5. A.F. Wang, J.J. Ying, Y.J. Yan, R.H. Liu, X.G. Luo, Z.Y. Li, X.F. Wang, M. Zhang, G.J. Ye, P. Cheng, Z.J. Xiang, X.H. Chen, Superconductivity at 32 K in single-crystalline $Rb_xFe_{2?y}Se_2$. Phys. Rev. B **83**, 060512 (2011)

6. J.T. Park, G. Friemel, Y. Li, J.-H. Kim, V. Tsurkan, J. Deisenhofer, H.-A. Krug von Nidda, A. Loidl, B. Keimer, D.S. Inosov, Magnetic resonant mode in the low-energy spin-excitation spectrum of superconducting single crystals. Phys. Rev. Lett. **107**, 177005 (2011)
7. V. Svitlyk, D. Chernyshov, E. Pomjakushina, A. Krzton-Maziopa, K. Conder, V. Pomjakushin, V. Dmitriev, Temperature and pressure evolution of the crystal structure of $A_x(Fe_{1-y}Se)_2$ (A = Cs, Rb, K) studied by synchrotron powder diffraction. Inorg. Chem. **50**, 10703 (2011)
8. M. Wang, M.Y. Wang, G.N. Li, Q. Huang, C.H. Li, G.T. Tan, C.L. Zhang, H.B. Cao, W. Tian, Y. Zhao, Y.C. Chen, X.Y. Lu, B. Sheng, H.Q. Luo, S.L. Li, M.H. Fang, J.L. Zarestky, W. Ratcliff, M.D. Lumsden, J.W. Lynn, P.C. Dai, Antiferromagnetic order and superlattice structure in nonsuperconducting and superconducting $Rb_yFe_{1.6+x}Se_2$. Phys. Rev. B **84**, 194504 (2011)
9. V. Tsurkan, J. Deisenhofer, A. Guenther, H.-A. Krug von Nidda, S. Widmann, A. Loidl, Phys. Rev. B **84**, 144520 (2011)
10. S. Bosma, R. Puzniak, A. Krzton-Maziopa, M. Bendele, E. Pomjakushina, K. Conder, H. Keller, S. Weyeneth, Magnetic-field tuned anisotropy in superconducting $Rb_xFe_{2-y}Se_2$. Phys. Rev. B **85**, 064509 (2012)
11. M. Gooch, B. Lv, L.Z. Deng, T. Muramatsu, J. Meen, Y.Y. Xue, B. Lorenz, C.W. Chu, High-pressure study of superconducting and nonsuperconducting single crystals of the same nominal composition $Rb_{0.8}Fe_2Se_2$. Phys. Rev. B **84**, 184517 (2011)
12. H.K. Onnes, The resistance of pure mercury at helium temperatures. Phys. Lab. Univ. Leiden **12**, 120 (1911)
13. J. Bardeen, Two-fluid model of superconductivity. Phys. Rev. Lett. **1**, 399 (1958)
14. H. Eyring, M. Polanyi, Über Einfache Gasreaktionen? Zeit. Phys. Chem. B 12, 279 (1931) H. Eyring, The activated complex in chemical reactions? J. Chem. Phys. **3**, 107 (1935)
15. H. Eyring, G.E. Kimball, J. Walter, *Quantum Chemistry* (Wiley, New York, 1944)
16. H. Eyring, Viscosity, plasticity, and diffusion as examples of absolute reaction rates. J. Chem. Phys. **4**, 283 (1936)
17. F.H. Ree, T.S. Ree, T. Ree, H. Eyring, Random walk and related physical problems. Adv. Chem. Phys. **4**, 1 (1962)
18. C.W. Kwang-Hua, Effect of activation volume on the defect-induced superconductivity in semiconducting superlattices. J. Solid State Chem. **192**, 179 (2012)
19. C.W. Kwang-Hua, Effect of defects on the pressure-induced transitional electronic transport in $TbTe_3$ and $ZrTe_3$. Chem. Phys. **409**, 37 (2012)
20. C.W. Kwang-Hua, Effect of activation volume on the pressure-induced anomalous resistances in $EuFe_2As_2$. Chem. Phys. **415**, 186 (2013)
21. Y.g. Oh, M.S. Jhon, H. Eyring, Significant structure theory applied to liquid helium-3. PNAS (USA) 74, 4739 (1977)
22. R. Ryoo, M.S. John, H. Eyring, Temperature and pressure dependence of viscosity of quantum liquid He-4 according to significant structure theory. PNAS (USA) 77, 4399 (1980)
23. W.A.B. Evans, G. Rickayzen, On the equivalence of the phenomena of the Meissner effect and infinite conductivity in superconductors. Ann. Phys. (NY) 33, 275 (1965)
24. V.Z. Kresin, S.A. Wolf, Inhomoneous superconducting state and intrinsic Tc: Near room temperature superconductivity in the cuprates. arXiv:1109.0341
25. S.V. Borisenko, A.N. Yaresko, D.V. Evtushinsky, V.B. Zabolotnyy, A.A. Kordyuk, J. Maletz, B. Bühner, Z. Shermadini, H. Luetkens, K. Sedlak, R. Khasanov, A. Amato, A. Krzton-Maziopa, K. Conder, E. Pomjakushina, H-H. Klauss, E. Rienks, "Cigar" Fermi surface as a possible requisite for superconductivity in iron-based superconductors. arXiv:1204.1316
26. J. Echeverría, S. Alvarez, Application of symmetry operation measures in structural inorganic chemistry. Inorg. Chem. **47**, 10965 (2008)
27. W. Bronger, A. Kyas, P. Müller, The antiferromagnetic structures of KFeS2, RbFeS2, KFeSe2, and RbFeSe2 and the correlation between magnetic moments and crystal field calculations. J. Solid State Chem. **70**, 262 (1987)